Journal of Applied Polymer Science

Photostabilization of polystyrene/montmorillonite nanocomposite. A Factorial Experimental Design 2^4

Camila F. P. Oliveira,[1] Silvio R. Cremm,[2] Gerson H. S. Cruz,[2] Guilhermino J. M. Fechine[2]

[1]Escola Politécnica – Universidade de São Paulo, São Paulo, SP, Brazil

[2]Escola de Engenharia, Universidade Presbiteriana Mackenzie, São Paulo, SP, Brazil

Correspondence to: G. J. M. Fechine (E-mail: guilherminojmf@mackenzie.br)

ABSTRACT: The weathering behavior of polystyrene (PS) and PS/montmorillonite nanocomposite with and without addition of ultraviolet (UV) absorber and/or antioxidant was investigated. Samples were exposed to UV radiation in the laboratory for periods of up to approximately 12 weeks. The samples were exposed for various irradiation intervals, and their tensile and impact strength was monitored through a factorial experimental design 2^4. The molecular weight, yellowness, and fracture surface were also monitored. The results generated by analysis of variance (ANOVA) Table showed that UV absorber and exposure time had the most important effects positive and negative, respectively. These results could be seen for neat PS and PS/MMT nanocomposite. The presence of antioxidant alone did not have any significant effect but when mixed with UV absorber presented a small synergism. These results corroborate with molecular weight, yellowing and fracture surface of tensile and impact samples. © 2012 Wiley Periodicals, Inc. J. Appl. Polym. Sci. 000: 000–000, 2012

KEYWORDS: photodegradation; photostabilization; nanocomposite; factorial design

Received 11 January 2012; accepted 4 June 2012; published online
DOI: 10.1002/app.38143

INTRODUCTION

In recent years, polymer clay nanocomposites studies have attracted a great interest from academic groups and industries, because they often exhibit excellent properties when compared with neat polymers.[1–7] In the case of polystyrene (PS) nanocomposites, the addition of very small quantities of nanoparticles on the PS matrix leads to a great improvement on mechanical properties, thermal, and fire properties of PS.[8,9] Nevertheless, little is known on the behavior of these materials when exposed to ultraviolet (UV) radiation.[10,11] Pollicin and coworkers[11] studied the influence of montmorillonite (MMT) nanodispersion on PS photo-oxidation using only infrared spectroscopy [Fourier transform infrared (FTIR) spectroscopy] to follow degradation process. The samples films (100 μm) were prepared by compression molding. They noticed that the rate of photo-oxidation of PS/MMT (organomodified or not MMT) was faster than the neat PS and suggested that the photo-oxidation instability could be related to degree of exfoliation and then to the presence of catalytic active sites on the MMT layer surface. Fechine and coworkers[10] analyzed the photo-oxidative behavior of PS-MMT nanocomposites using size exclusion chromatography (SEC), FTIR, mechanical properties (tensile and impact), and scanning electron microcopy (SEM). In this case, the samples used were prepared by injection molding (dimensions according to ASTM, thickness $\cong$ 3.0 mm). Nonexposed samples presented a decrease of mechanical properties with increasing filler content; however, during the photodegradation, the composites showed an improved performance. This behavior can be attributed to a screen effect against UV radiation and barrier effect against diffusion of oxygen promoted by MMT particles. The difference between the results obtained by thin films and thick samples is due the oxygen availability. Whereas in thin films the oxygen is available all the time in whole sample, thick samples have a gradient of available oxygen from the surface to the center that depends of diffusivity of oxygen.

In some applications, it is not desired that polymers degrade very quickly. The photodegradation and photostabilization mechanisms of most polymers are well-known,[12–25] however, there are only few studies on polymeric composites.[25–30] Most of these publications about polymer nanocomposite photostabilization used thin films as samples. Chemical modifications and molecular weight have been used as tools to evaluate the degradation mechanism. As said before, the rate of photo-oxidation is completely different for thick samples, and a lot of questions still remained about mechanical properties and fracture surface of the samples exposed to UV radiation. In this work, it was evaluated the photostabilization of PS and PS/MMT clay nanocomposites by adding an UV absorber and/or antioxidant. The nanocomposites were prepared using melt mixing techniques. Fechine and coworkers[10] evaluated the clay content on PS/MMT composite and verified that 2.5 wt

% conducted to obtain an exfoliated nanocomposite as seen on X-ray diffraction and transmission electron microscopy. Samples were produced with 2.5 wt % of commercial MMT clay (Cloisite 15 A). The sample bars were exposed to UV radiation in a Q-Lab weathering chamber for periods of up to 12 weeks. To evaluate the effects of presence of clay (MMT), UV absorber (UV), antioxidant (ANT), and exposure time (TIME) on mechanical properties (tensile and impact), a 2^4 factorial experimental design with five replications in a total of 80 runs was used. After 12 weeks of the exposure, the extension of degradation was also evaluated by scanning electronic microscopy (SEM), size exclusion chromatography (SEC) and yellowness.

EXPERIMENTAL

Materials

In this work, commercial PS — PS N1841 from Innova (MFI = 11 g/10 min – 200°C/5 kg) was used. According to the manufacturer, the polymer did not contain UV stabilizers. The organophilic clay used was Cloisite 15 A from Southern Clay Products. It is a MMT modified with a saturated quaternary ammonium cation (dimethyl, dihydrogenated tallow ammonium). A hindered phenol antioxidant [see the Figure 1(a)] and an UV absorber [see Figure 1(b)] were used as additives. The nanocomposites were prepared using a melt mixing technique. The materials were prepared in a mixing chamber attached to a torque rheometer (Thermo Haake's PolyLab 900/Rheomix 600 p). The polymer was mixed with the clay at 200°C at a rotor speed of 50 rpm for 7 min. The clay fractions were fixed at 2.5 wt % and the concentration of antioxidant and UV absorbers was fixed at 0.5% (w/w). Samples for mechanical testing were prepared by injection molding. The injection-molded bars were produced using a DEMAG injection-molding machine with dimensions according to ASTM D638 and D256 for tensile and impacts tests, respectively.

Photooxidation Conditions

The sample exposures were conducted in a Q-Lab weathering chamber using Q-Panel UVA fluorescent lamps. These lamps are 1.2 m long and produce UV light that matches reasonably well with sunlight with a cut-off at 290 nm. The weathering cycle was defined as follows: 8 h under UV light at 60°C and 4 h in the dark under condensed water at 50°C. The irradiation intensity reaching the sample surface is 0.89 W/m^2. Under these conditions, the specimens are submitted to a combination of photo-, thermal and hydrolytic degradation, offering very harsh conditions to the sample deterioration.

Characterization

For tensile properties measurements, the samples were tested in a Kratos K 2.000MP machine operating with a crosshead speed of 20 mm/min at 25°C. For Izod impact properties measurements, the samples were tested in a Tinius Olsen IT 504 machine at 25°C. The values of tensile strength, maximum elongation, and impact strength reported here represent averages for at least five samples. After tensile testing, the fracture surfaces of the specimens were observed using a Phillips XL30 Scanning Electron Microscope operating at 15–20 kV. The samples were sputtered with a gold layer to avoid charging problems.

After various exposure times, the samples were analyzed by SEC. SEC analyses were conducted in a Viscoteck with a series

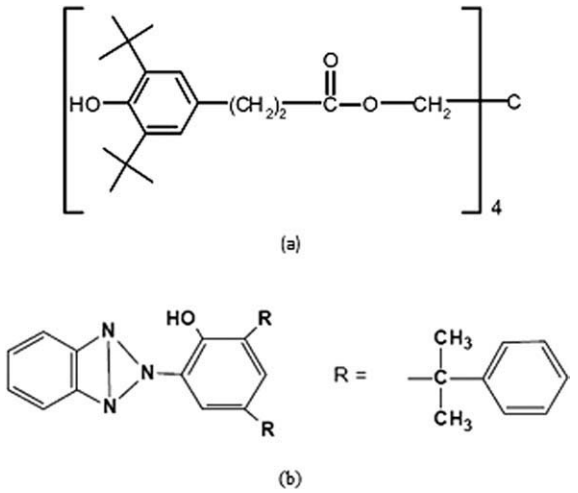

Figure 1. Chemical Structure of Antioxidant (a) and UV absorber (b).

of columns at 40°C and with a refractive index detector. Specimens for SEC were taken from a depth on 1 mm of the UV-exposed surface, dissolved in THF, and the filtered solution was injected into the equipment. The solvent flow rate (THF) was 1 mL/min and the columns were calibrated with narrow molecular weight PS. The average number of chain scission per macromolecule was determined using the following equation:

$$\text{Number of scissions} = \frac{\bar{M}_{n_0}}{\bar{M}_{n_t}} - 1 \qquad (1)$$

$\bar{M}_{n_0}$ and $\bar{M}_{n_t}$ denote the number average molecular weight of the material unexposed and exposed to UV radiation for 12 weeks, respectively.

The yellowness was monitored by change of coloration of the impact samples observed from digital images. The images were taken using a digital photography machine with 3.5 MPixel of the resolution.

Factorial Experiment Design

To evaluate the effects of clay content, UV absorber content, antioxidant content, and exposure time on mechanical properties (tensile and impact), it was used a 2^4 factorial experimental design with five replications in a total of 80 runs leading to a value of degree of freedom equal to 79. Statistical data treatment was performed by Statistica 5.0 software (StatSoft) and was based on the analysis of variance (ANOVA). ANOVA Table produces relevant values like the mean squares (MS) [eq. (3)] of the independent variables, their interaction, and residual. MS values were calculated from the sum of squares (SS) [eq. (2)] divided by the degrees of freedom (df). *F*-test (square of effects/squares of residual) and *P*-value (significance probability) [eq. (4)] were calculated to evaluate the significance effects. The *P*-value represents the probability to obtain a specific value in the *F* distribution with k-1 variables and $k(n$-1) df higher or equal to F_0 (k is the population number and n is the sample size). With the *P*-value, it is possible to evaluate if the dependent variables are significant, how significant, and their interaction. The significance level (α) for the global statistical treatment was set to 0.05, which

Table I. Factor Levels of the Independent Variables used for Evaluation of PS/MMT Photostabilization

Independent variable	Label	Low (−1)	High (+1)
Clay content (wt %)	x	0.0	2.5
UV absorber content (wt %)	y	0.0	0.5
Antioxidant content (wt %)	z	0.0	0.5
Exposure time (weeks)	w	0.0	12

is typically used as standard value for 2^4 factorial experiments collected in five replications. From these values and degrees of freedom, it is possible to obtain F_0 value from a reference table. If the calculated F value is higher than the F_0 value, the represented effect is considered statistically relevant. The independent variable intervals used in this work are shown in Table I. The dependent variables are impact strength, stress at the break point, strain at the break point. Surface response equations are expressed only in terms of relevant dependent variables.

$$SS = \sum_{i=1}^{n}\sum_{j=1}^{n}\left(x_{ij} - 1/nk\sum_{i=1}^{n}\sum_{j=1}^{n}x_{ij}\right)^2 \quad (2)$$

$$MS = SS/df \quad (3)$$

$$P - \text{value} = P[F(k-1), k(n-1) > F_0] \quad (4)$$

RESULTS AND DISCUSSION

All composites showed worse mechanical properties than neat PS corroborating the studies of several authors.[31–34] PS does not usually have strong interactions with clay and its tensile strength is normally decreased on addition of clay as the clay particles can act as stress concentrators. The study presented here has no interest in producing a composite with better mechanical properties than neat PS, however, would only evaluate the photodegradation and photostabilization processes of PS/MMT composite.

Factorial Design 2^4

For the most important anticipated applications, the significant properties and dependent variables of evaluation of PS/MMT photostabilization are (i) impact strenght, (ii) stress at the break point, and (iii) strain at the break point. These properties represent the statistical responses that were evaluated against the key independent variables of the process: (i) clay content, (ii) UV absorber content, (iii) antioxidant content, and (iv) exposure time. For optimization purposes, a 2^4 factorial experimental design was used.

Table II lists the raw data of the responses obtained for each combination of factors where the high and low value for each factor is coded as +1 and −1, respectively. Table II also shows data from SEC analysis. Table III shows the main effects of independent variables and their respective combinations, and the Table IV shows the significance level of all dependent variables through F-test and P-values. If the F value for a given effect is higher than the F_0 (F-theoretical), this effect is significant. An independent variable has a significant influence whenever the P-value is lower than 0.05. The main effect shown in Table III represents the improvement obtained by changing the factor level of the independent variables from low to high. Although the sign of the effect indicates an increase (when positive) or decrease (when negative) of the parameter, its absolute value indicates the total change observed.

Table II. Crude Results for all Limits of the Independent Variables and SEC Data

Variable limits[a] x, y, z, w	Impact strength (J/m)	Stress at the break point (MPa)	Strain at the break point (%)	$\overline{M}_n$ (g/mol)	$\overline{M}_w$ (g/mol)	PD[b]	NS[c]
+1, +1, +1, +1	88.33 ± 2.86	36.02 ± 3.05	3.35 ± 0.23	41,200	94,800	2.30	0.31
+1, +1, +1, −1	89.43 ± 1.67	39.32 ± 0.62	3.19 ± 0.14	53,900	76,500	1.40	–
+1, +1, −1, +1	93.05 ± 3.54	38.12 ± 1.61	2.94 ± 0.10	36,000	92,100	2.56	0.54
+1, +1, −1, −1	86.61 ± 1.67	38.85 ± 1.24	3.41 ± 0.03	55,600	79,800	1.44	–
+1, −1, +1, +1	18.12 ± 7.97	19.34 ± 1.70	1.79 ± 0.23	21,600	62,000	2.87	1.83
+1, −1, +1, −1	89.45 ± 1.14	39.49 ± 0.54	3.06 ± 0.16	61,200	86,800	1.42	–
+1, −1, −1, +1	14.83 ± 2.83	15.91 ± 0.88	1.61 ± 0.08	19,000	59,800	3.15	1.83
+1, −1, −1, −1	91.21 ± 3.36	38.11 ± 1.98	3.34 ± 0.13	53,700	99,700	1.86	–
−1, +1, +1, +1	101.53 ± 15.46	43.31 ± 0.56	3.57 ± 0.10	46,000	97,800	2.13	0.24
−1, +1, +1, −1	130.01 ± 8.80	42.64 ± 0.62	3.54 ± 0.15	57,100	78,500	1.37	–
−1, +1, −1, +1	100.75 ± 14.00	42.41 ± 1.86	3.78 ± 0.16	40,600	89,900	2.21	0.46
−1, +1, −1, −1	119.79 ± 10.23	43.43 ± 2.18	3.73 ± 0.25	59,200	85,300	1.44	–
−1, −1, +1, +1	27.96 ± 5.44	22.62 ± 1.73	1.85 ± 0.21	23,300	65,000	2.79	1.51
−1, −1, +1, −1	128.97 ± 10.53	43.57 ± 0.52	3.77 ± 0.08	58,400	84,900	1.45	–
−1, −1, −1, +1	24.38 ± 6.22	15.43 ± 1.01	1.56 ± 0.12	23,300	67,700	2.91	1.87
−1, −1, −1, −1	122.49 ± 6.77	43.97 ± 0.80	3.87 ± 0.10	66,800	104,800	1.57	–

[a]See Table I for label value and limit value, [b]PD = $\overline{M}_n/\overline{M}_w$, [c]NS = number of scissions.

Table III. Results for Main Effects for all Independent Variables and Its Interactions

	Main effects		
	Impact strength	Stress at the break point	Strain at the break point
Clay content (*x*)	−22.98	−4.02	−0.41
UV absorber content (*y*)	36.63	10.70	0.80
Antioxidant content (*z*)	2.46	1.26	−0.05
Exposure time (*w*)	−48.75	−12.03	−0.97
x − *y*	−0.43	−0.84	−0.09
x − *z*	−2.81	−0.47	0.01
x − *w*	12.91	0.43	0.07
y − *z*	−0.44	−1.64	−0.07
y − *w*	37.95	10.93	0.84
z − *w*	−1.72	1.10	0.14
x − *y* − *z*	−0.67	0.03	0.07
x − *y* − *w*	0.06	−1.35	−0.24
x − *z* − *w*	1.36	−1.22	0.05
y − *z* − *w*	−2.26	−1.31	0.07

As seen in Tables III and IV, UV absorber content (*y*) is the most important positive parameter on the photostabilization of PS/MMT nanocomposite. This statement is based on the higher value of the effect combined with lower *P*-value (equal to zero) together with the highest *F* values on all independent variables. The value of UV absorber content effect is the highest positive number compared with the others parameters alone. These results confirm the positive effect of UV absorber during the exposition to UV radiation of neat polymers and nanocomposite polymers showed by others authors before.[10,35] On the other hand, clay content (*x*) and exposure time (*w*) are the most negative parameters on the photostabilization of PS/MMT nanocomposite. These affirmations were also based on values showed in Tables III and IV. When the "*y*" parameter is combined with the others, it also shows good results. A good example of that is the combination of the "*y*" and "*w*" that change the negative effect of exposure time (*w*) to positive effect on impact strength, stress, and strain at the break point; −48.75 to 37.95, −12.03 to 10.93 and −0.97 to 0.84, respectively. The antioxidant content (*z*) has no significance on photostabilization of neat PS and PS/MMT nanocomposite according to Tables III and IV.

Some explanations have been made about the best and worst significant parameters on photostabilization of PS/MMT according to main effects, *F*-estimated and *P*-value. The factorial designer used is a good tool to understand if the UV absorber has the same power on photostabilization of PS neat and PS/MMT nanocomposite. This is possible through of the interactions of the independent variables. The values of "*y*", "*y* − *w*," and "*x* − *y* − *w*" for impact strength are 36.63, 37.95, and −0.06; for stress at the break point are 10.70, 10.93, and −1.35; for stress at the break point are 0.80, 0.84 and −0.24, respectively. The "*y*" and "*y* − *w*" positive values mean that the UV absorber act very well on PS neat; however, when the clay is inserted, "*x* − *y*− *w*," the power of UV absorber is decreased to negative value for all independent variables. These results show that the power of UV absorber is not the same on presence of clay. Recent researches have revealed two types of phenomena: In thin films (∼100 μm), there is the catalytic effect of iron impurities of nanoclays on polymer photo-oxidation[11,35,36]; however, in thick samples,

Table IV. *F*-test[a] and Significance Probability (*P-value*) for all Dependent Variables: Impact Strength, Stress at the Break Point and Strain at the Break Point

	F-estimated/*P*-value		
	Impact strength	Stress at the break point	Strain at the break point
Clay content (*x*)	179.87/0.00	159.18/0.00	139.81/0.00
UV absorber content (*y*)	457.02/0.00	1125.84/0.00	528.57/0.00
Antioxidant content (*z*)	2.06/0.15	15.52/0.00	2.45/0.12
Exposure time (*w*)	809.45/0.00	1422.06/0.00	791.49/0.00
x − *y*	0.06/0.80	7.03/0.01	7.73/0.01
x − *z*	2.68/0.11	2.14/0.15	0.01/0.98
x − *w*	56.76/0.00	1.83/0.18	3.77/0.06
y − *z*	0.06/0.80	26.31/0.00	4.72/0.03
y − *w*	490.65/0.00	1174.64/0.00	587.94/0.00
z − *w*	1.02/0.32	11.85/0.00	17.61/0.00
x − *y* − *z*	0.15/0.70	0.01/0.92	4.18/0.00
x − *y* − *w*	0.01/0.97	17.97/0.00	48.38/0.00
x − *z* − *w*	0.62/0.43	14.70/0.00	2.28/0.13
y − *z* − *w*	1.75/0.20	17.06/0.00	3.94/0.05

[a]F theoretical (F_0) = 3.9 for $\alpha = 0.05$ and degrees freedom total (df) = 79.

$$M^{n+} + POOH \rightarrow M^{(n+1)} + PO^{\bullet} + HO^{-}$$

$$M^{(n+1)} + POOH \rightarrow M^{n+} + POO^{\bullet} + H^{+}$$

Scheme 1. Hydroperoxide decomposition reactions catalyzed by metallic ions.

there is a screen effect against UV radiation and barrier effect against diffusion of oxygen promoted by MMT particles.[10] The results about the influence of clay content "x" (−22.98) and the interaction with exposure time "$x - w$" (12.91) on impact strength confirm the last sentence about screen and barrier effects for thick samples. The results showed on Tables I and II indicate that even if the MMT particles help to protect the polymer against UV radiation, on the other hand, they promote the decreasing of the UV absorber power, probably due to hydroperoxides decomposition catalyzed by iron from nonoclays (see Scheme 1).

Molecular Weight

Table II shows data from SEC analysis for all samples. It is important to remember that the samples for SEC analysis were taken from exposed face directly to UV radiation (1 mm of depth). After 12 weeks of exposition to UV radiation, all samples show a decreasing of molecular weight (number average molecular weight, $\overline{M}_n$, and weight average molecular weight, $\overline{M}_w$) with an increasing of polydispersity. This is polymer characteristic that undergoes degradation by molecular scissions. The interesting point is to know how much was the decreasing in molecular weight. An indication of that is taken from the number of scissions. For neat PS, the values for PS without additives, PS + UV absorber, PS + antioxidant, and PS + UV absorber + antioxidant were 1.87, 0.46, 1.51, and 0.24, respectively. These results also indicate that the UV absorber protect the PS against UV radiation and a synergism effect when the two additives are used. The same behavior can be seen for PS/MMT nanocomposite. The synergism was not found on mechanical properties, probably, because the result from these analyses depend not only the surface characteristics but also the whole sample.

The main idea was using the antioxidant to protect the PS during the processing, consequently, become less sensible to UV radiation. The results of molecular weight showed that the antioxidant at 0.5% (w/w) could not protect the PS during the processing. The $\overline{M}_n$ of neat PS was around 67,000 g/mol and the nonexposed PS + antioxidant has a value of the 59,000 g/mol. When the phenolic antioxidants are used as a sole additive in polymer system without any filler or secondary antioxidant heterolysing hydroperoxide, scavenge polymer peroxy radicals and convert them to hydroperoxides under simultaneous formation of phenoxy radicals. The final result is that no hydroperoxides are removed from the oxidation process.[37]

Nonexposed PS/MMT samples showed a less molecular weight ($\overline{M}_n$ = 53,700 g/mol) than nonexposed PS/MMT + antioxidant one ($\overline{M}_n$ = 61,200 g/mol). Kumar et al.[38] have already showed that the antioxidant alone is usually used to stabilize polymers during the processing, mainly when there is some catalyze agent on composition. The molecular weight results found that the antioxidant could inhibit the catalyze effect of the iron present on nanoparticules. In the case of the photostabilization, all results showed that the antioxidant alone did not showed any significant effect. Probably, during the processing, an amount of antioxidant had been consumed, and the remaining content was not enough to help on photostabilization alone. A small effect could be noticed when the antioxidant was mixed with UV absorber. For the UV absorber, all results demonstrating that its presence reaches good levels of photostability.

Yellowness

The Figure 2 shows the images from the nonexposed PS and PS/MMT samples and others samples exposed to 12 weeks. The yellowness of PS has been extensively studied[39] and the change of coloration during the photodegradation is related to carbonyl groups generating by absorption of UV radiation and oxygen (see Scheme 2). As can see on Figure 2, PS after 12 weeks of exposure changes its color to transparent for very intense yellow

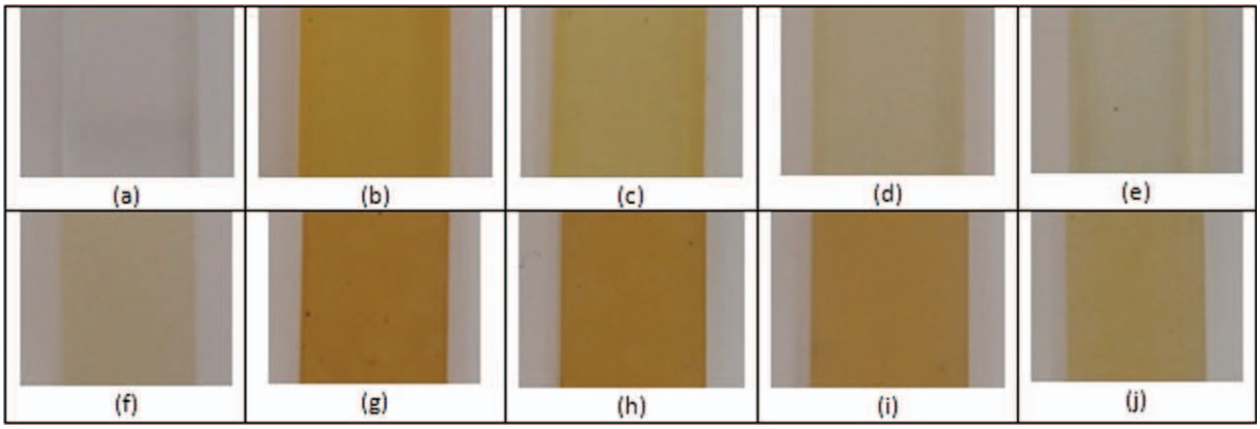

Figure 2. The color of the neat PS nonexposed (a), exposed PS for 12(b), exposed PS + antioxidant for 12(c), exposed PS + UV absorber for 12(d), and exposed PS + antioxidant + UV absorber for 12(e) weeks; the color of the nonexposed PS/MMT (f), exposed PS/MMT for 12(g), exposed PS/MMT + antioxidant for 12(h), exposed PS/MMT + UV absorber for 12(i), and exposed PS/MMT + antioxidant + UV absorber for 12(j) weeks. [Color figure can be viewed in the online issue, which is available at wileyonlinelibrary.com.]

Applied Polymer SCIENCE

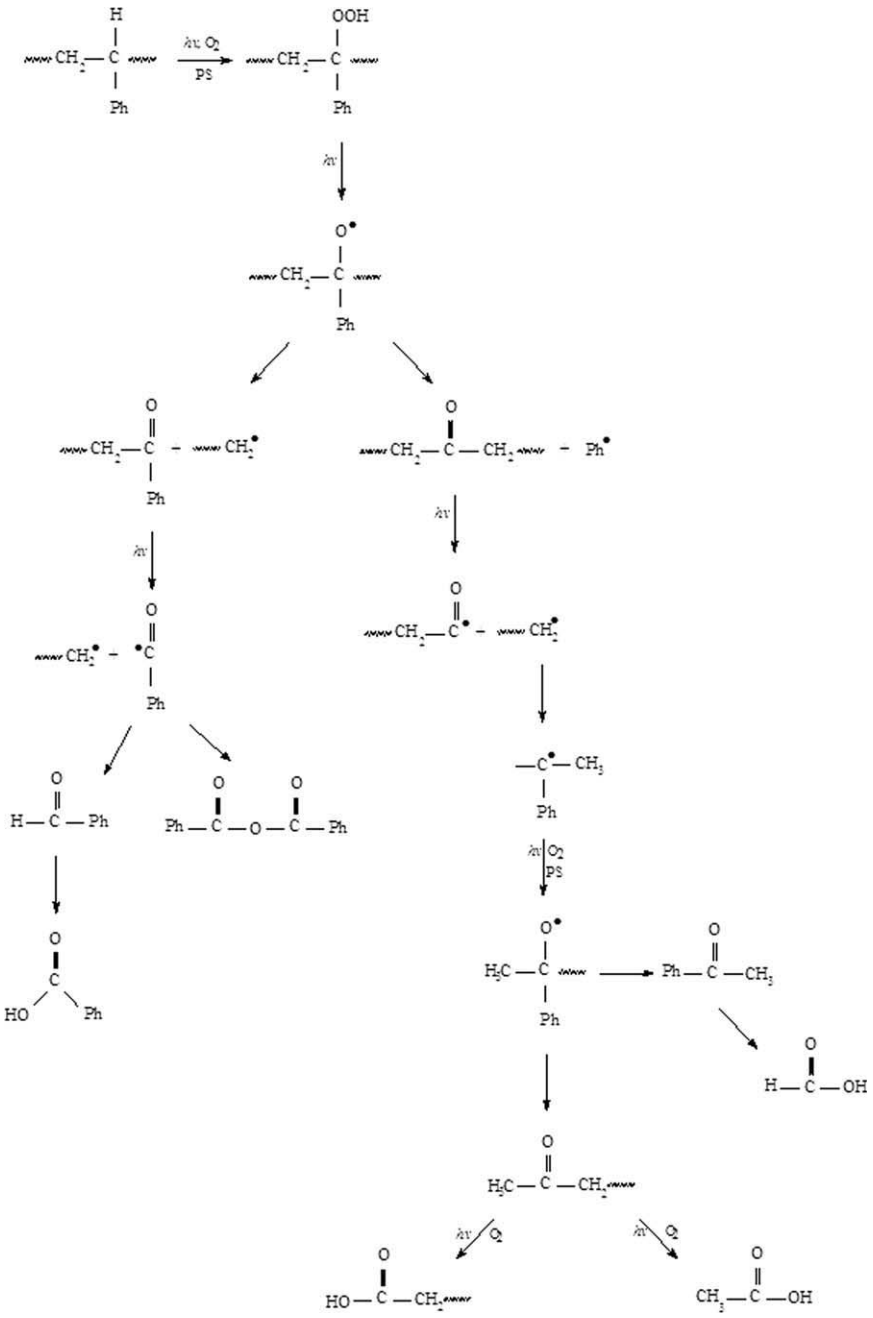

Scheme 2. Photodegradation mechanism of PS.[3]

[Figure 2(b)]. The intensity of the yellowness was decreased when the antioxidant and UV absorber was added, mainly when both of them were together. One of the actions of the antioxidant is to capture the free radical generating on the first step of the photo-oxidant process; and the UV absorber hinders the UV radiation absorption from the polymer. It is clear that the prevention of the yellowness is achieved by the presence of these additives. The PS/MMT samples were also protected by the additives at the same way.

Fracture Surface Analysis

Impact Surface Fracture. Figure 3 shows the fracture surface of impact PS samples, with and without additives, nonexposed and exposed to UV radiation for 12 weeks. The nonexposed PS shows a fracture surface typical of brittle polymers without large deformation. First, a craze is formed by separation between adjacent molecules. This region is called "mirror" zone (flat fracture), and it is followed by rougher surface usually called "hackle" which is associated with bifurcation and branching of the crack [Figure 3(a)]. The first zone is characterized by moderate velocity of propagation and high level of fracture surface energy (FSE) unlike the second region that occurs at high velocity of propagation and lower values of FSE.[40,41]

The fracture surface of exposed PS is different from the one of nonexposed PS. The fracture initiates at a site near to the edge

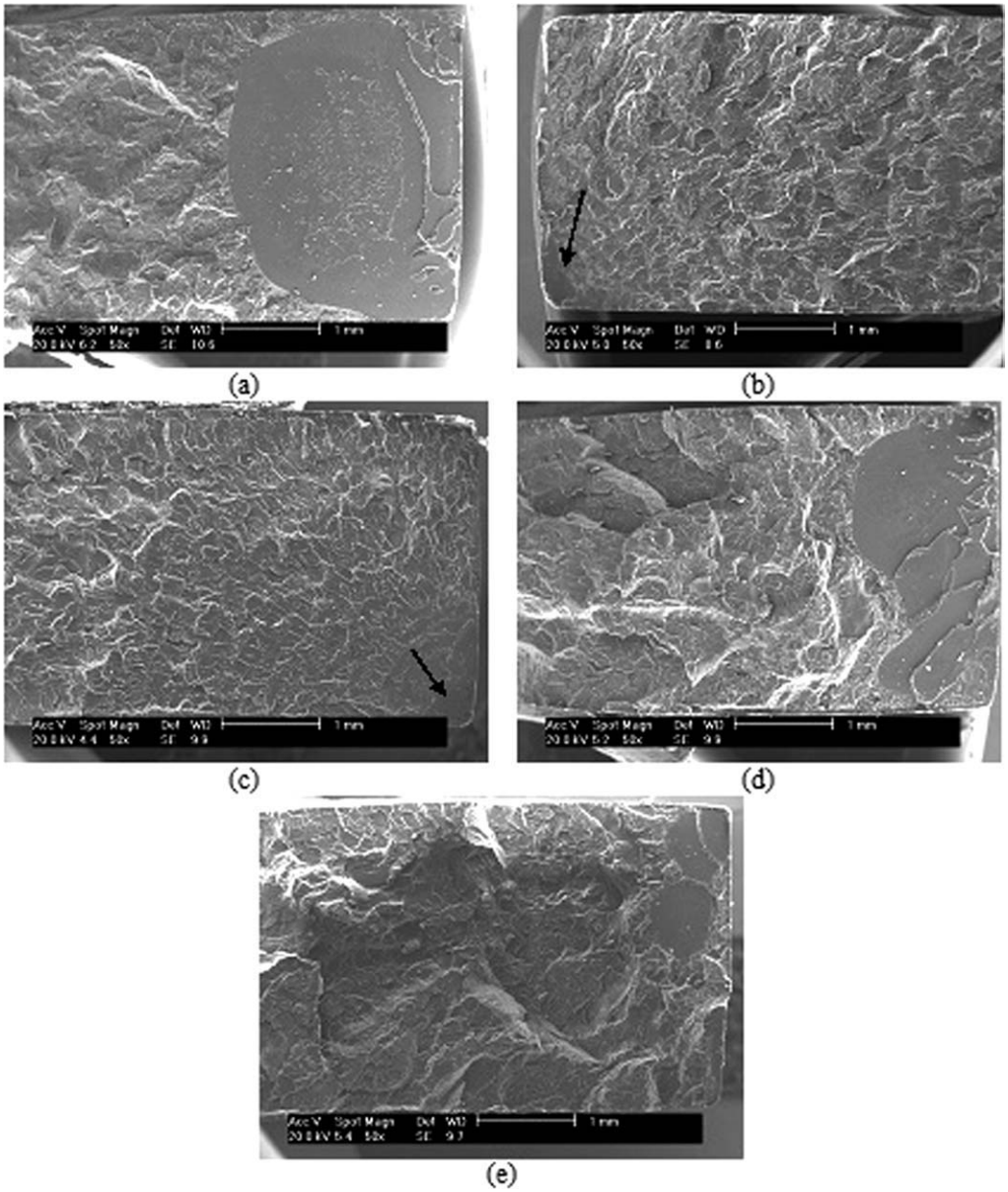

Figure 3. Impact fracture surfaces of the neat PS nonexposed (a), exposed PS for 12 (b), exposed PS + antioxidant for 12 (c), exposed PS + UV absorber for 12 (d), and exposed PS + antioxidant + UV absorber for 12 weeks (e).

[see the arrow on Figure 3(b)] as a consequence of the embrittlement due to the decrease in molecular weight. The decreasing of molecular weight is higher on surface because in this place, the oxygen is more available than in deeper places. The fracture surface is characterized by crack propagation at high velocity without a "mirror" zone. The topography of this region (crack propagation) is smooth when compared with the same region of the nonexposed PS sample. Low level of FSE is correlated to this kind of surface fracture. The same fragile fracture surface can be seen on PS + antioxidant sample exposed to 12 weeks [Figure 3(c)], whereas PS + UV absorber and PS + UV absorber + antioxidant samples keep the characteristic of PS nonexposed [Figures 3(d,e), respectively]. These results corroborate with the impact strength showed on Table II and with the factorial design analysis.

Nonexposed PS/MMT fracture surface (Figure 4(a)) is characterizing by a decrease of the "mirror" zone due to the presence of the clay particles that acting as stress concentrators. The nanoclay particles may in fact act as defects within PS matrix under applied loads and consequently become sites for cracking and subsequent fracture. It corroborates with the crude impact strength data on Table II when the values for neat PS samples are higher than PS/MMT nanocomposites ones. After 12 weeks, the PS/MMT sample without any additives [Figure 4(b)] shows a flatter topography with fracture initiated near to face exposed directly to UV radiation. Low level of FES characterizes this kind of fracture. The PS/MMT + antioxidant sample exposed to 12 weeks shows the same behavior. PS/MMT samples with UV absorber and UV + antioxidant show a rougher topography similar to PS/MMT samples nonexposed. These results also

Applied Polymer SCIENCE

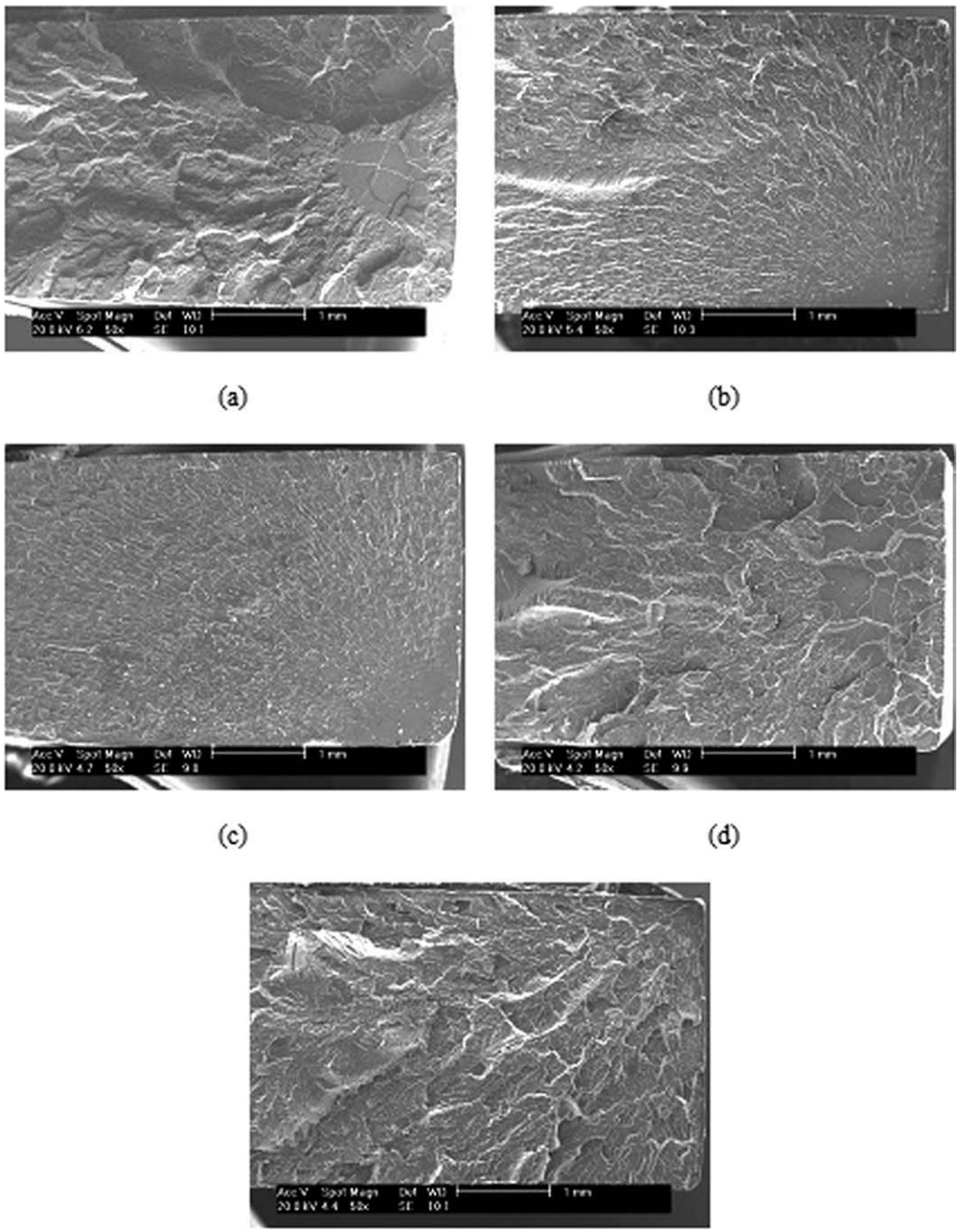

Figure 4. Impact fracture surfaces of the PS/MMT nonexposed (a), exposed PS/MMT for 12 (b), exposed PS/MMT + antioxidant for 12 (c), exposed PS/MMT + UV absorber for 12 (d), and exposed PS/MMT + antioxidant + UV absorber for 12 weeks (e).

confirm the data from Table II for impact strength and factorial design analysis.

Tensile Surface Fracture. Figure 5 shows the fracture surface of tensile PS samples, with and without additives, nonexposed and exposed to UV radiation for 12 weeks. The fracture surface of neat PS shows that the unexposed PS had a fracture surface typical of brittle polymers without deformation bands or extensive orientation[42] [Figure 5(a)]. After 12 weeks of exposure, the fracture surface changes completely [Figure 5(b)]. The craze starts from the degraded surface of the sample in a unique flat plane followed by cracking propagation at higher velocities then brittle fracture occurs along the craze boundaries.[40,41] The consequence of that is the decrease of stress and strain at the break point, as seen on crude data on Table II. The same behavior happens with PS + antioxidant sample, as seen on Figure 5c. The PS + UV absorber [Figure 5(d)] and PS + UV absorber + antioxidant (Figure 5(e)) samples show a thin degradable layer near to surface. However, these samples keep the same fracture characteristic of nonexposed PS. These images confirm the results obtained on tensile tests.

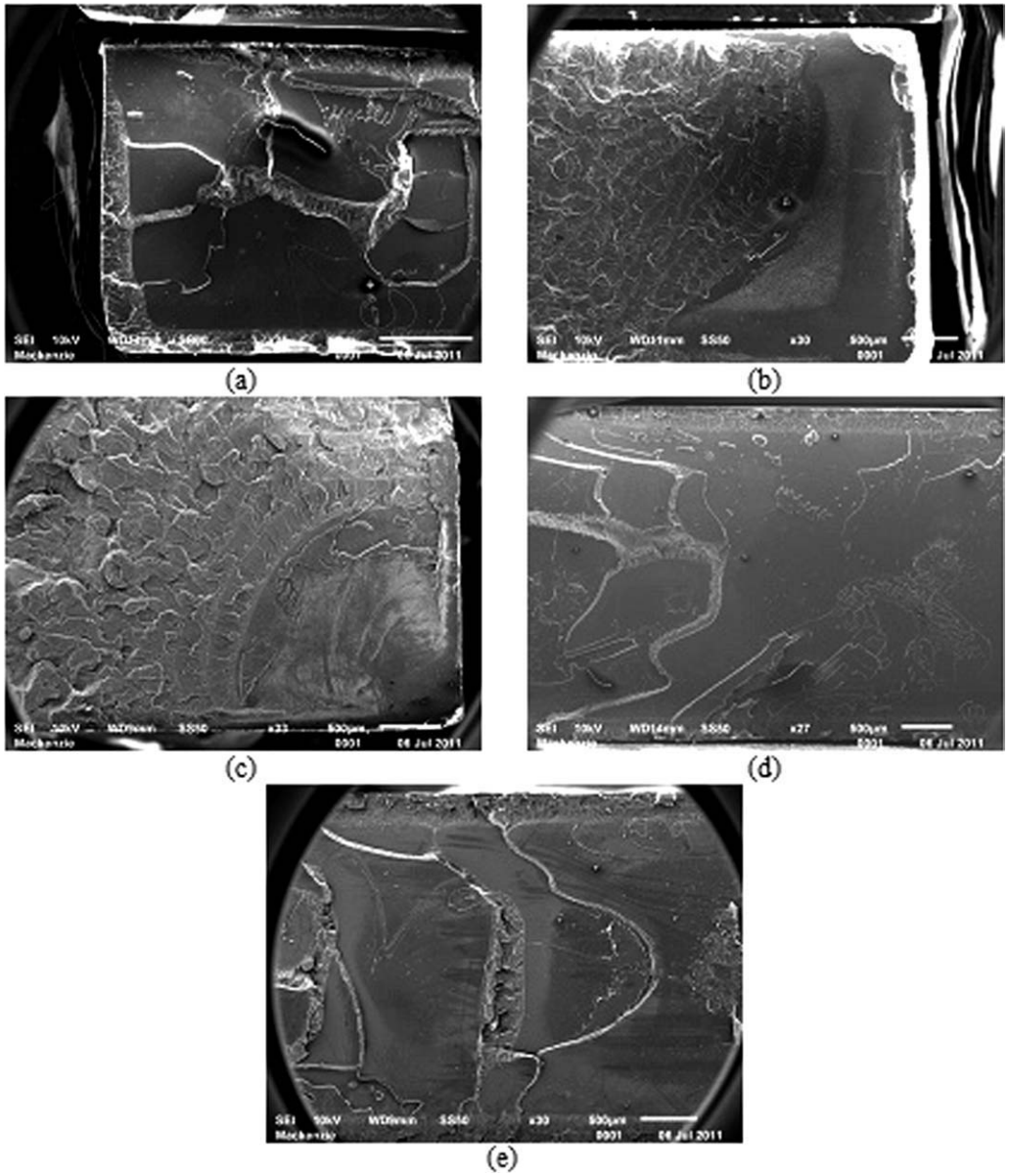

Figure 5. Tensile fracture surfaces of the neat PS nonexposed (a), exposed PS for 12 (b), exposed PS + antioxidant for 12 (c), exposed PS + UV absorber for 12 (d), and exposed PS + antioxidant + UV absorber for 12 weeks (e).

The addiction of MMT particles changed the surface fracture of the samples when compared with neat PS [Figure 6(a)]. PS does not usually have strong interactions with particles and its tensile strength is normally decreased on addition of clay as the clay particles can act as stress concentrators. Lower values of the stress and strain at the break point are observed because of this phenomenon. After 12 weeks of exposure, PS/MMT sample exhibits a spot when the crack start [see the arrow on Figure 6(b)] followed by fast propagation where a smooth topography is seen. It could be also seen on PS/MMT + antioxidant sample [Figure 6(c)]. This kind of topography is characterized by low levels of FSE. PS/MMT + UV absorber [Figure 6(d)] and PS/MMT + UV absorber + antioxidant [Figure 6(e)] samples show a similar fracture surface of nonexposed PS/MMT sample consequently close values of the stress and strain at the break point.

CONCLUSIONS

The photostabilization of neat PS and PS-MMT nanocomposites was analyzed using a factorial designer 2^4. Some techniques were used to evaluate the photodegradation process: SEC, change of color, mechanical properties (tensile and impact), and SEM. The photostabilization of the polymers could be done using several additives, however, the type and content varies according to the chemical structure of the polymer and the fillers present in the polymer. The factorial designer helps to understanding the real effect of the additives used in this work and showed that UV absorber (TINUVIN 234) was very efficient and the antioxidant only had a small significant effect when used with UV absorber. Different from the others researches, here, we studied the photostabilization of the thick

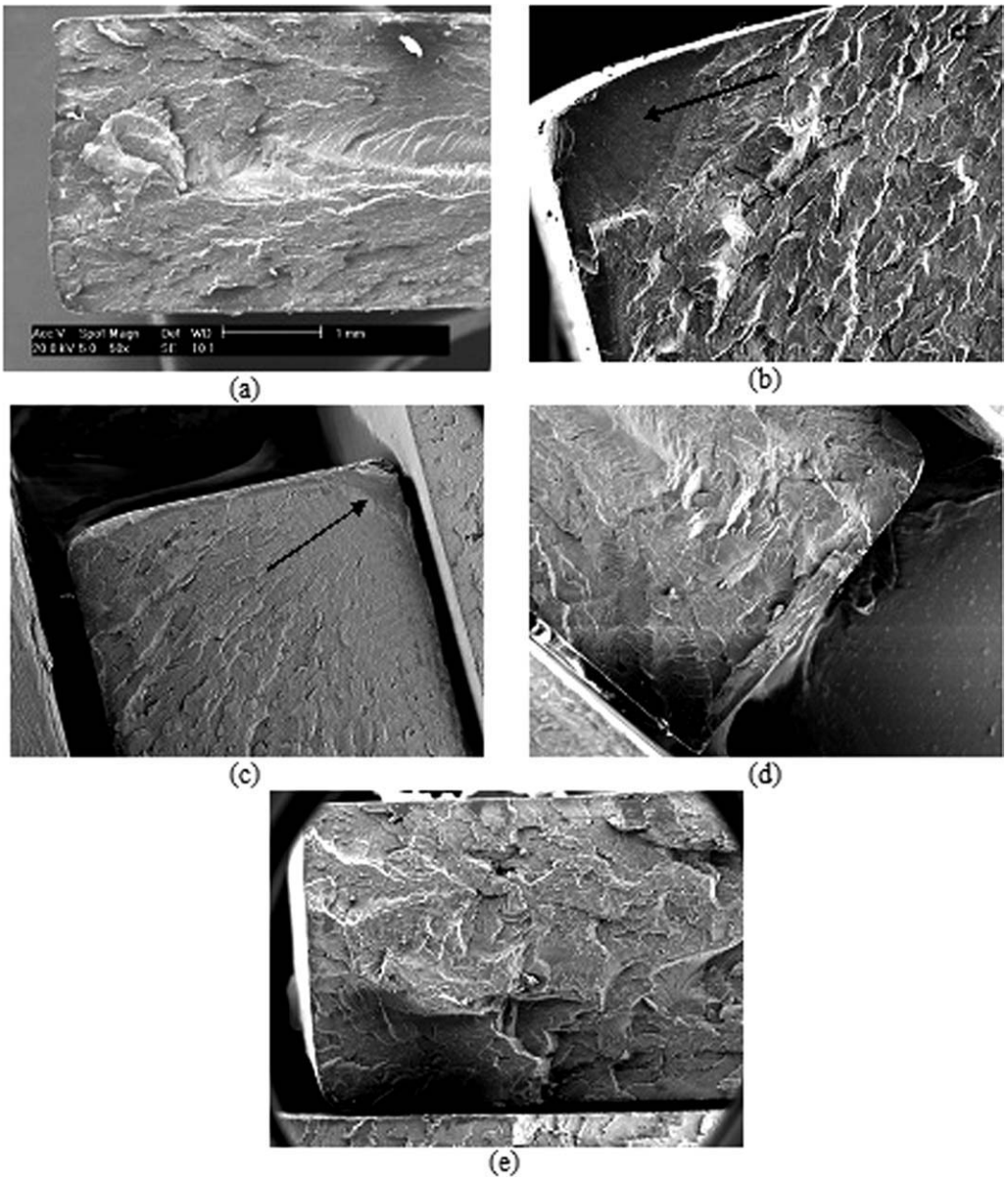

Figure 6. Tensile fracture surfaces of the PS/MMT nonexposed (a), exposed PS/MMT for 12 (b), exposed PS/MMT + antioxidant for 12 (c), exposed PS/MMT + UV absorber for 12 (d), and exposed PS/MMT + antioxidant + UV absorber for 12 weeks (e).

samples and the analysis of the fracture surface were very important to elucidate what happened on bulk of these samples.

ACKNOWLEDGMENTS

The authors would like to thank the Fundação de Amparo a Pesquisa do Estado de São Paulo – FAPESP for financial support.

REFERENCES

1. Samir, M. A. S. A.; Alloin, F.; Dufresne, A. *Biomacromolecules* **2005,** *6*, 612.
2. Lee, Y. H.; Lee, J. H.; An, I.; Kim, C.; Lee, D. S.; Lee, Y. K.; Nam, J. *Biomaterials* **2005,** *26*, 3165.
3. Someya, Y.; Sugahara, Y.; Shibata, M. *J. Appl. Polym. Sci.* **2005,** *95*, 386.
4. Chigwada, G.; Wang, D.; Wilkie, C. A. *Polym. Degrad. Stab.* **2006,** *91*, 848.
5. Ray, S. S.; Okamoto, M. *Prog. Polym. Sci.* **2003,** *28*, 1539.
6. Ray, S. S.; Okamoto, M. *Macromol. Mater. Eng.* **2003,** *288*, 936.
7. Grunert, M.; Winter, W. T. *J. Polym. Environ.* **2002,** *10*, 27.
8. Wang, B. N.; Wikie, C. A. *Polymer* **2005,** *46*, 2933.
9. Yei, D. R.; Kuo, S. W.; Su, Y. C.; Chang, F. C. *Polymer* **2004,** *45*, 2633.
10. Oliveira, C. F. P.; Carastan, D. J.; Demarquette, N. R.; Fechine, G. J. M. *Polym. Eng. Sci.* **2006,** *48*, 1511.

11. Bottino, F. A.; Di Pasquale, G.; Fabbri, E.; Orestano, A.; Pollicin, A. *Polym. Degrad. Stab.* **2009,** *94*, 369.
12. Rabello, M. S.; White, J. R. *Plast. Rubber Compos.* **1996,** *25*, 237.
13. Carlsson, D. J.; Wiles, D. M. *J. Macromol. Sci. - Rev. Macromol. Chem.* **1976,** *C14*, 65.
14. Rabello, M. S.; White, J. R. *Polym. Degrad. Stab.* **1997,** *56*, 55.
15. Allen, N. S. *Eng. Plast.* **1995,** *8*, 247.
16. Rabello, M. S.; White, J. R. *J. Appl. Polym. Sci.* **1997,** *64*, 2505.
17. Girois, S.; Audouin, L.; Verdu, J.; Delprat, P.; Marot, G. *Polym. Degrad. Stab.* **1996,** *51*, 125.
18. Fechine, G. J. M.; Rabello, M. S.; Souto-Maior, R. M. *Polym. Degrad. Stab.* **2002,** *75*, 153.
19. Rabello, M. S.; Tocchetto, R. S.; Barros, L. A.; D'Almeida, J. R. M.; White, J. R. *Plast. Rubber Compos.* **2001,** *30*, 132.
20. Fechine, G. J. M.; Rabello, M. S.; Souto-Maior, R. M. *J. Material Sci.* **2002,** *37*, 4979.
21. Fechine, G. J. M.; Rabello, M. S.; Catalani, L. H. *Polymer* **2004,** *45*, 2303.
22. Gugumus, F. *Polym. Degrad. Stab.* **1995,** *50*, 101.
23. Allen, N. S.; Edge, M.; Corrales, T.; Catalina, F. *Polym. Degrad. Stab.* **1998,** *61*, 139.
24. Seliger, H.; Happ, E.; Cascaval, A.; Birsa, L.; Nicolaescu, T.; Poinescu, T.; Cojocariu, C. *Eur. Polym. J.* **1999,** *35*, 827.
25. Cho, S.; Choi, W. *J. Photochem. Photobiol. A: Chem.* **2001,** *143*, 221.
26. Leong, Y. W.; Abu Bakar, M. B.; Ishak, Z. A. M.; Ariffin, A. *Polym. Degrad. Stab.* **2004,** *83*, 411.
27. Maia, D. R. J.; Balbinot, L.; Poppi, R. J.; De Paoli, M. A. *Polym. Degrad. Stab.* **2003,** *82*, 89.
28. Ansari, D. M.; Price, G. J. *Polymer* **2004,** *45*, 1823.
29. Stark, N. M.; Matuana, L. M. *Polym. Degrad. Stab.* **2004,** *86*, 1.
30. Selden, R.; Nystron, B.; Langstrom, R. *Polym. Compos.* **2004,** *25*, 543.
31. Hasegawa, N.; Okamoto, H.; Kawasumi, M.; Usuki, A. *J. Appl. Polym. Sci.* **1999,** *74*, 3359.
32. Wang, D.; Zhu, J.; Yao, Q.; Wilkie, C. A. *Chem. Mater.* **2002,** *14*, 3837.
33. Seper, M.; Utracki, L. A.; Zheng, X.; Wilkie, C. A. *Polymer* **2005,** *46*, 11569.
34. Su, S.; Jiang, D. D.; Wilkie, C. A. *Polym. Degrad. Stab.* **2004,** *83*, 333.
35. Morlat-Therias, S.; Fanto, E.; Gardette, J.; Dintcheva, N. T.; La Mantia, F.; Malatesta, V. *Polym. Degrad. Stab.* **2008,** *93*, 1776.
36. Lonkar, S. P.; Kumar, A. P.; Singh, R. P. *Polym. Adv. Technol.* **2007,** *18*, 891.
37. Marek, A.; Kapralkova, L.; Schmidt, P.; Pfleger, J.; Humlicek, J.; Pospisil, J.; Pilar, J. *Polym. Degrad. Stab.* **2006,** *91*, 444.
38. Kumar, A. P.; Depan, D.; Tomer, N. S.; Singh, R. P. *Prog. Polym. Sci.* **2009,** *34*, 479.
39. Rabek, J. F. Polymer photodegradation; Chapman & Hall: London, **1995**
40. Doyle, M. J. *J. Mater. Sci.* **1975,** *10*, 300.
41. Doyle, M. J. *J. Mater. Sci.* **1973,** *8*, 1185.
42. Souza, A. R.; Amorin, K. L. E.; Medeiros, E. S.; Mélo, T. J. A.; Rabello, M. S. *Polym. Degrad. Stab.* **2006,** *91*, 1504.